Collisional quenching of CO $B\,^1\Sigma^+(v'=0)$ probed by two-photon laser-induced fluorescence using a picosecond laser

F. Di Teodoro,[a] J. E. Rehm, R. L. Farrow, and P. H. Paul
Combustion Research Facility, Sandia National Laboratories, Livermore, California 94551

(Received 15 May 2000; accepted 25 May 2000)

We report measurements of room-temperature, species-specific quenching cross sections of CO $B\,^1\Sigma^+$ $(v'=0)$ in collisions with He, Ne, H_2, N_2, Ar, CO, Kr, CH_4, O_2, Xe, CO_2, C_3H_8, and H_2O. The measured quenching cross sections (in $Å^2$) were 0.25 ± 0.02, 0.54 ± 0.04, 11.0 ± 0.4, 24.6 ± 0.5, 27.7 ± 0.5, 37 ± 2, 42 ± 2, 81 ± 4, 85 ± 5, 99 ± 6, 133 ± 5, 144 ± 7, and 170 ± 8, respectively. Two-photon excitation of the CO molecules via the Hopfield–Birge system ($X\,^1\Sigma^+ \rightarrow\rightarrow B\,^1\Sigma^+$) was performed using the frequency-tripled 690 nm emission of a custom-built picosecond dye laser. Blue-to-green fluorescence in the Angström bands ($B\,^1\Sigma^+ \rightarrow A\,^1\Pi$) was detected using a microchannel-plate photomultiplier tube and recorded with a digital storage oscilloscope. The quenching cross sections were directly obtained by time resolving the temporal decay of the fluorescence signal and observing its variation as a function of the quencher pressure. The effect of radiative trapping on the observed fluorescence was also quantitatively modeled. © *2000 American Institute of Physics.* [S0021-9606(00)02332-1]

I. INTRODUCTION

Detecting CO in multicomponent reacting flows such as plasmas and flames is important in numerous research fields, including planetary atmospheric physics, biochemistry, surface science, and combustion diagnostics. Laser-induced fluorescence (LIF) detection of CO by two-photon exciting the Hopfield–Birge electronic transition ($X\,^1\Sigma^+ \rightarrow \rightarrow B\,^1\Sigma^+$) and collecting blue-to-green emission in the Angström bands ($B\,^1\Sigma^+ \rightarrow A\,^1\Pi$) was first demonstrated by Loge *et al.*[1] This technique is receiving considerable development for applications in combustion.[2–16] The analysis of two-photon LIF for quantitatively determining CO concentrations requires a detailed knowledge of the rate of collisional quenching of the $B\,^1\Sigma^+$ state, which can be calculated only if the cross sections for quenching by all collision partners are known. A direct and accurate way to obtain quenching cross sections is to time resolve the fluorescence signal after short-pulse laser excitation and observe the variation of the fluorescence lifetime as a function of the quencher pressure. As discussed in Sec. IV, CO $B\,^1\Sigma^+$ has a natural lifetime of about 22 ns and collisions with even modest pressures (<1 Torr) of strongly quenching species (e.g., water vapor) reduce the effective fluorescence lifetime to a few nanoseconds. Thus, excitation by standard ~10 ns pulse dye lasers is impractical for time-resolved studies. This problem has been circumvented in some cases[1,17,18] by resorting to Stern–Volmer methods,[19] which extract the quenching cross sections from the pressure dependence of the time-integrated fluorescence. However, these methods can be unreliable if the fluorescence decay is nonexponential,[20] if radiative trapping occurs, or if the excited transition has non-negligible pressure broadening.[17] To our knowledge, only Agrup and Aldén presented a time-resolved study of two-photon LIF from CO $B\,^1\Sigma^+$.[9,10] Although they reported a measurement of the CO self-quenching rate coefficient, the principal objective of their work was to measure the $B\,^1\Sigma^+$-state lifetime in hydrocarbon flames. Therefore, species-specific quenching cross sections were not obtained.

In this article, we report the use of a picosecond laser and a detection apparatus with subnanosecond response time to induce and temporally resolve the Angström-band fluorescence in mixtures of CO with several quenching gases at room temperature. Species-specific quenching cross sections for CO $B\,^1\Sigma^+$ $(v'=0)$ in collisions with major combustion species (H_2O, C_3H_8, CO_2, CH_4, O_2, H_2, and N_2) and noble gases (He, Ne, Ar, Kr, and Xe) are determined directly from the pressure dependence of the fluorescence. The pressures of the CO/quencher mixtures are chosen such that the fluorescence signal is well described by a single-exponential function with a characteristic time much longer than the instrumental response time. The measured quenching cross sections are found to span ~3 orders of magnitude. The CO self-quenching cross section is also obtained with the aid of a radiation-trapping model. By fitting parameters of the model to observed fluorescence lifetimes, we further obtain the $B\,^1\Sigma^+$ $(v'=0)$-state radiative lifetime along with branching ratios and Einstein coefficients for the $B\,^1\Sigma^+ \rightarrow A\,^1\Pi$ and $B\,^1\Sigma^+ \rightarrow X\,^1\Sigma^+$ fluorescence channels. We have compared our results for H_2, N_2, He, Ne, and Ar to those of previous studies based on Stern–Volmer methods, while quenching of CO $B\,^1\Sigma^+$ $(v'=0)$ by the other species is reported here for the first time to our knowledge.

The article is organized as follows: in Sec. II, we describe the laser system and experimental apparatus; in Sec. III, a model giving the dynamics of the excited-state population in the presence of quenching and radiation trapping is introduced; in Sec. IV, we report the measured species-

[a]Electronic mail: fditeod@ca.sandia.gov

specific quenching cross sections of CO $B\,^1\Sigma^+$ $(v'=0)$ and use the previously developed model to characterize the self-quenching; in Sec. V, we discuss the interpretation of our results in terms of possible quenching mechanisms; finally, in Sec. VI, we summarize our findings and suggest directions for future work.

II. EXPERIMENT

The experimental setup consisted of a picosecond dye laser, a cell, and a fluorescence detection/recording apparatus. The picosecond dye laser was in-house built; a complete description and analysis of its performance will be the subject of a future publication. For brevity, we provide here only a short description of its design. We used the second harmonic (532 nm) of a regenerative Nd:YAG amplifier (Positive Light, ~100 ps pulse duration, 20 Hz repetition rate, ~1 W output power) seeded by an actively mode-locked laser (Lightwave Electronics series 131, ~100 ps pulse duration, 100 MHz repetition rate, 1064 nm wavelength, ~150 mW output power) to transversely pump a broadband oscillator formed by the opposing windows of a flowing dye cell containing a solution of LDS 698 dye in methanol. The oscillator output pulses had a measured duration somewhat shorter than the ~100 ps width of the pump laser, but were spectrally broad (20 nm FWHM, centered at about 692 nm). The spectral bandwidth was reduced to 0.8 cm^{-1} using a transmission filter consisting of a holographic diffraction grating (2700 g/mm) at grazing incidence, a collimating lens, a slit, and two mirrors. The filter design is based on the time-compensated filter of Hung *et al.*,[21] which does not temporally broaden the filtered pulses while ensuring excellent passive wavelength stability. Following amplification in two side-pumped dye cells, we obtained pulse durations of ~85 ps and pulse energies up to 6 mJ. With frequency tripling in BBO crystals, pulse energies up to 0.4 mJ could be obtained at 230 nm, with a bandwidth <1.5 cm^{-1}. We maintained a typical pulse energy of about 100 μJ for most measurements, except for those required to determine the CO self-quenching as explained in Sec. IV.

The laser beam was focused onto the center of a stainless-steel cell equipped with fused-silica entrance and exit windows and a quartz side window. The cell was evacuated to $\sim 8\times10^{-6}$ Torr with a turbomolecular pump prior to each measurement session. All gases used were originally reagent grade and were further purified with gas-chromatograph filters: we used oxygen getters (Matheson 6406-A) to individually purify inert gases and CO, while molecular sieves (Matheson 451) were used for the other species. The pressure of the mixtures was monitored with capacitance manometers.

The fluorescence light was collected through the side window at a 90° angle from the cell axis, spectrally filtered by two color glasses (Melles-Griot SWP610 and GG395) to select the Angström-band emission in the wavelength range 400–600 nm, and focused on the photocathode of a microchannel-plate photomultiplier tube (Hamamatsu R7024U, 350 ps fall time). For the self-quenching measurements (which required increasing the CO pressure and, therefore, the emitted fluorescence intensity) we placed several absorptive-type neutral density filters before the photomultiplier tube to avoid saturating the detector. The signal was, finally, observed and recorded using a digital storage oscilloscope (Tektronix TDS 680B, 1 GHz bandwidth).

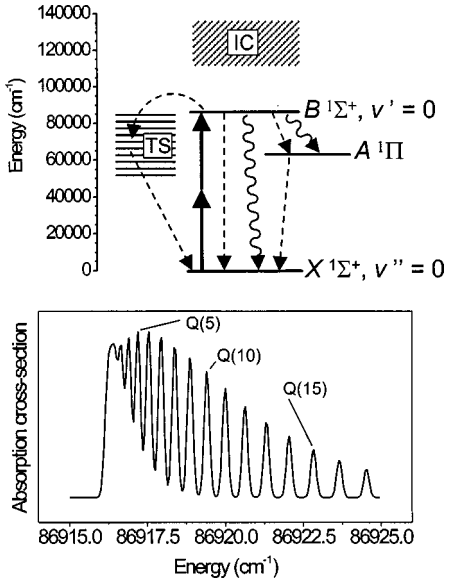

FIG. 1. Upper panel: relevant energy levels and excitation scheme; thick solid arrows: laser excitation; wavy arrows: fluorescence emission; dashed arrows: quenching paths; IC: ionization continuum; TS: triplet states. Lower panel: theoretical two-photon absorption cross section for the Q branch of the $X\,^1\Sigma^+(v''=0)\rightarrow\rightarrow B\,^1\Sigma^+(v'=0)$ transition in 10 mTorr of CO at 295 K.

During the study of CO self-quenching, blue-to-green stimulated emission (SE) was observed after the cell exit window along the propagation direction of the pumping laser beam (see Sec. IV). The SE beam was spectrally separated from the laser beam using appropriate color filters, detected with a PIN silicon photodiode (Electro-Optics Technology ET2000, falltime <350 ps), and monitored with the same digital oscilloscope.

We also monitored, for each quencher species, the collision-induced fluorescence from triplet states of CO in the wavelength range 260–360 nm (see Sec. V A). This fluorescence was observed by blocking the Angström-band fluorescence with a color glass (UG11).

III. THEORY

The energy levels relevant to this experiment are schematically illustrated in Fig. 1. The CO molecules are two-photon pumped from the $X\,^1\Sigma^+$ $(v''=0)$ ground state to the $B\,^1\Sigma^+$ $(v'=0)$ state predominantly through Q-branch transitions.[22–24] The excited state can radiatively decay through the $B\rightarrow A$ and $B\rightarrow X$ channels. As can be seen from the theoretical spectrum[25] of the two-photon absorption cross section in Fig. 1, several J' levels are comprised within the spectral bandwidth of our laser.[26] Thus, the detected intensity, $I_f(t)$, of the undispersed $B\rightarrow A$ fluorescence can be written as

$$I_f(t)\propto\sum_v\sum_{J,J'}\int_V \hbar\omega^v_{J',J}A^v_{J',J}\Omega n_{J'}(\mathbf{r},t)d_3\mathbf{r}, \tag{1}$$

where the vibrational quantum number v ranges approximately from 0 to 4 (Angström bands at 451 and 608 nm, respectively); $J=J'$, $J'\pm1$; V is the observation volume; $\omega^{v}_{J'J}$ and $A^{v}_{J'J}$ are the angular frequency and the Einstein coefficient for the $B\,^1\Sigma^+$, $v'=0$, $J'\rightarrow A\,^1\Pi$, v, J transition; Ω is the detection solid angle; and $n_{J'}(\mathbf{r},t)$ is the J'-level population at time t and location $\mathbf{r}$ in the cell. The time evolution of $n_{J'}$ is, in general, determined by the concomitant action of laser excitation, photoionization (attained via the absorption of a third 230 nm photon), rotational thermalization, predissociation, SE, spontaneous emission, radiation trapping, and electronic quenching. Laser excitation and photoionization are temporally confined within the ~100 ps pulse duration and, therefore, have no influence on the signal observed after the response time of the detection system. We will neglect the predissociation which is known to affect only rotational levels with $J'>37$.[23] As discussed by Westblom *et al.*,[8] the $B\rightarrow A$ SE can provide an additional deactivation channel for the excited state and perturb the early-time evolution of the observed fluorescence signal, introducing difficulties in interpretation. However, it can be minimized by reducing the pump intensity, as discussed in Sec. IV and, therefore, will not be included in the present model.

While the J' dependence of the radiative lifetime has been shown to be negligible,[27] no data is available for the J' dependence of the quenching rates of CO $B\,^1\Sigma^+$. According to Eq. (1), a J'-dependent quenching would cause $I_f(t)$ to depart from a single-exponential decay because the dynamics of distinct J'-state populations, $n_{J'}(\mathbf{r},t)$, would be different.[28] However, the detected fluorescence signal consistently exhibited a single-exponential decay, unless significant SE occurred. Thus, we can rewrite Eq. (1) as

$$I_f(t)\propto\int_V n(\mathbf{r},t)d^3\mathbf{r},$$

where $n(\mathbf{r},t)$ is a rotationally averaged $B\,^1\Sigma^+$ $(v'=0)$-state population.

Most of the $B\rightarrow X$ fluorescence (undetected in these studies) is emitted in the (0, 0) band, which has a near-unity Franck–Condon factor.[29] As a result, the $B\rightarrow X$ fluorescence can be absorbed by vibrationless ground-state CO molecules, a process known as radiation trapping.[30] Note that only the $B\rightarrow X$, rather than the $B\rightarrow A$, fluorescence is trapped in this experiment because the absorption of the emitted fluorescence occurs predominantly outside the small region irradiated by the laser beam and is, therefore, due to molecules with negligible population in the A state. By performing the measurements in a pressure regime where the pulse duration is much shorter than the observed decay time of the excited state, the dynamics of $n(\mathbf{r},t)$ can be described by the Holstein equation[31] modified to include quenching and branching of the emitted fluorescence:

$$\frac{\partial n(\mathbf{r},t)}{\partial t}=-\left(\frac{1}{\tau_{\rm rad}}+Q\right)n(\mathbf{r},t)+\frac{\beta}{\tau_{\rm rad}}\mathcal{L}n(\mathbf{r},t). \tag{2}$$

Here, $\tau_{\rm rad}$ is the radiative lifetime of the excited state, Q is the rotationally averaged quenching rate, β is the branching ratio for the $B\rightarrow X$ fluorescence channel ($\beta\equiv\tau_{\rm rad}A_{B\rightarrow X}$, $A_{B\rightarrow X}$ being the Einstein coefficient for the $B\rightarrow X$ spontaneous emission), and $\mathcal{L}$ is an integral operator defined as

$$\mathcal{L}n(\mathbf{r},t)\equiv\int_V G(\mathbf{r},\mathbf{r}')n(\mathbf{r}',t)d\mathbf{r}',$$

where $G(\mathbf{r},\mathbf{r}')$ is the probability that a photon emitted at $\mathbf{r}'$ is reabsorbed at $\mathbf{r}$ and the integration is over the entire cell volume. The general solution of Eq. (2) can be written as[32]

$$n(\mathbf{r},t)=\sum_m \alpha_m\psi_m(\mathbf{r})\exp\left(-\frac{t}{g_m\tau_{\rm rad}}\right). \tag{3}$$

Here, the coefficients α_m depend on boundary and initial conditions, while g_m and $\psi_m(\mathbf{r})$ can be obtained by substituting Eq. (3) in Eq. (2), which reduces the Holstein equation to an eigenvalue problem for the operator $\mathcal{L}$,

$$\mathcal{L}\psi_m(\mathbf{r})=\left(\frac{Q\tau_{\rm rad}}{\beta}+\frac{1}{\beta}-\frac{1}{g_m\beta}\right)\psi_m(\mathbf{r}). \tag{4}$$

Note that $\mathcal{L}$ is, by definition, independent of quenching and unaffected by the branching of the fluorescence as long as only one branch of the fluorescence is trapped.[32] Hence, $\mathcal{L}$ is the same operator that would appear in the Holstein equation for a two-level system without quenching, namely the equation obtained from Eq. (4) by setting $Q=0$ and $\beta=1$:

$$\mathcal{L}\tilde{\psi}_m(\mathbf{r})=\left(1-\frac{1}{\tilde{g}_m}\right)\tilde{\psi}_m(\mathbf{r}). \tag{5}$$

As a result, the set of eigenfunctions obtained from Eqs. (4) and (5) must coincide [that is $\psi_m(\mathbf{r})=\tilde{\psi}_m(\mathbf{r})$ for every m] while g_m and $\tilde{g}_m$ are related by

$$g_m\tau_{\rm rad}=\left[\frac{1}{\tau_{\rm rad}}+Q-\frac{\beta}{\tau_{\rm rad}}\left(1-\frac{1}{\tilde{g}_m}\right)\right]^{-1}. \tag{6}$$

In a variety of experimental situations of interest, the first term $(m=0)$ in Eq. (3) dominates while higher-order terms represent fine corrections mainly affecting the early-time decay of the observed fluorescence signal. The actual number of terms to be taken into account is, however, best decided upon inspection of the temporal behavior of the fluorescence. The fluorescence decays that we analyzed were all well described by a single-exponential function over the entire CO pressure range under investigation (see also the discussion of Sec. IV). Thus, the series in Eq. (3) can be truncated to the lowest-order term by writing

$$n(\mathbf{r},t)\propto\psi_0(\mathbf{r})\exp\left(-\frac{t}{g_0\tau_{\rm rad}}\right).$$

Here, the ''trapping factor,'' g_0, has the physical meaning of the mean number of scattering events (absorption and reemission) suffered by a detected photon before leaving the cell. The *effective* lifetime of the fluorescing state, $g_0\tau_{\rm rad}$, is obtained via Eq. (6) from the solution of Eq. (5) for $m=0$. This problem has been the subject of intense study in the past and a variety of numerical techniques for its solution are available.[32] Moreover, several analytic approximations for

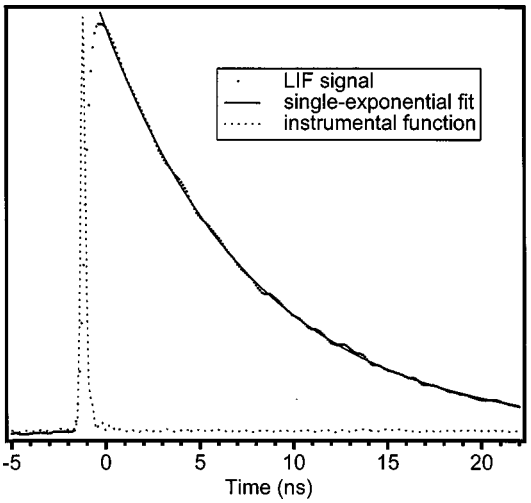

FIG. 2. Two-photon LIF signal from a CO/H_2O mixture (see the text).

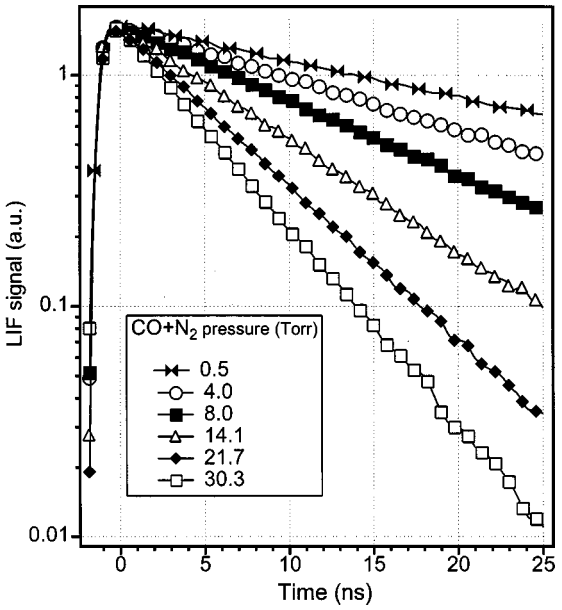

FIG. 3. Two-photon LIF signals from a CO/N_2 mixture at different total pressures and constant partial pressure (4 mTorr) of CO.

the dependence of $\tilde{g}_0$ on the medium opacity have been reported.[33] These analytic expressions are well suited for fitting purposes and are designed to agree with the predictions of *ab initio* Monte Carlo simulations of the radiative trapping process and direct numerical integrations of Eq. (2), for different experimental geometries, and for a wide opacity range. To model the pressure dependence of the fluorescence lifetime, we approximated $\tilde{g}_0$ with an analytic function appropriate for finite cylindrical cells and described in Ref. 34. There, Mölisch and co-workers observed that, for cell diameters and lengths comparable to ours, $\tilde{g}_0$ can be approximated by

$$\tilde{g}_0 \simeq 1+\left(\frac{1}{\tilde{g}_0^{\text{slab}}-1}+\frac{1}{\tilde{g}_0^{\text{cyl}}-1}\right)^{-1}, \tag{7}$$

where $\tilde{g}_0^{\text{slab}}$ and $\tilde{g}_0^{\text{cyl}}$ are analytic approximations for the trapping factors in the plane-parallel-slab and infinite-cylinder cell geometry, respectively:

$$\tilde{g}_0^{\text{slab,cyl}}=1+\frac{K}{2m_0^{\text{slab,cyl}}}\ln\left(\frac{K}{2}+e\right) - \frac{c_{0,0}^{\text{slab,cyl}}K\ln K+c_{1,0}^{\text{slab,cyl}}K+c_{2,0}^{\text{slab,cyl}}K^2}{1+c_{3,0}^{\text{slab,cyl}}K+c_{4,0}^{\text{slab,cyl}}K^2}.$$

Here, $m_0^{\text{slab,cyl}}$ and $c_{j,0}^{\text{slab,cyl}}$ are geometrical coefficients that have been tabulated in Ref. 32 and are kept constant in the fitting procedure, while K is the peak opacity of the medium at the center of the spectral distribution of the trapped fluorescence.

IV. RESULTS

The ability of our detection system to temporally resolve the emitted fluorescence is illustrated in Fig. 2, which shows a typical fluorescence signal (4 mTorr of CO diluted in about 2 Torr of water vapor) along with a single-exponential fit and the measured instrumental function. The instrumental function is obtained by observing Rayleigh scattering of the 230 nm laser pulse in ~500 Torr of argon and exhibits a full width at half maximum (FWHM) of about 900 ps. Figure 3 shows the variation of the fluorescence decay rate with the partial pressure of the quencher species (N_2 in this case). For a CO/quencher mixture, the quenching rate introduced in Eq. (2) can be written as

$$Q=q(P-P')+q'P', \tag{8}$$

where q and P are the quenching rate coefficient of the quenching species and the total pressure of the mixture, respectively, while q' and P' are the self-quenching rate coefficient and partial pressure of CO. Based on Eqs. (6) and (8), the decay rate, γ, of the fluorescence signal is given by

$$\gamma=\frac{1}{g_0\tau_{\text{rad}}}=q(P-P')+q'P'+\frac{1}{\tau_{\text{rad}}}-\frac{\beta}{\tau_{\text{rad}}}\left(1-\frac{1}{\tilde{g}_0}\right) =qP+C(P'). \tag{9}$$

Therefore, we recorded fluorescence signals from CO mixed with each individual quencher at several values of P and a constant P', as in the example of Fig. 3. We determined the decay rate at each P by means of a single-exponential fit. The resulting quencher-specific plots of γ vs P are presented in Fig. 4 along with linear fits, which, based on Eq. (9), provide the values of q reported in Table I. The related uncertainties were estimated from either the standard deviation over multiple measurements or the statistical error affecting the linear fit, whichever was larger. Finally, the thermally averaged quenching cross sections, σ, were derived using[19]

$$\sigma=\frac{q}{2}\sqrt{\frac{\pi\mu k_B T}{2}}, \tag{10}$$

where μ is the reduced mass of the CO/quencher system, k_B is Boltzmann's constant, and $T=294\pm1$ K is the temperature.

A different type of analysis was carried out to determine the CO self-quenching. Figure 5 shows the observed variation of the fluorescence lifetime as a function of P' in the

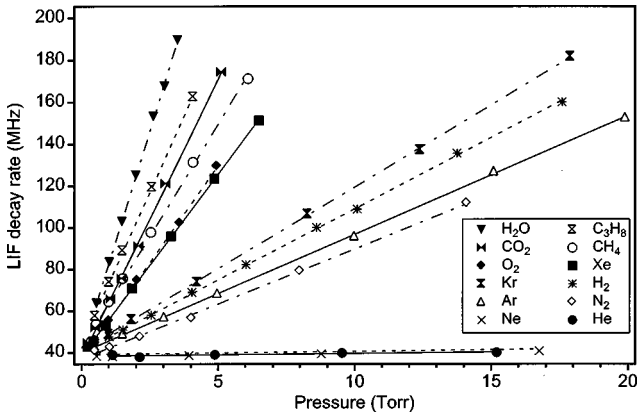

FIG. 4. Fluorescence decay rates as a function of the total pressure of the CO/quencher mixture. The straight lines passing through the data points are fits.

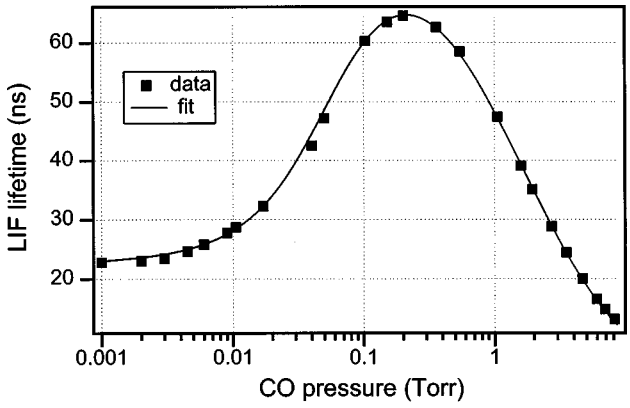

FIG. 5. Lifetime of the fluorescence emitted by pure CO as a function of the CO pressure. Solid line: the fit obtained from the model developed in Sec. III.

case of pure CO ($P=P'$), which reflects the interplay of radiation trapping and quenching. As expected, the lifetime increases initially with pressure from a nearly collision-free value of 22.8 ns ($P'=0.001$ Torr) to a strongly trapped value of about 65 ns ($P'=P'_{\max}\simeq 0.2$ Torr) due to the increasing opacity of the medium. At sufficiently high pressures, however, the self-quenching overcomes the trapping effect and causes the lifetime to decrease in a quasilinear fashion. Precautions were necessary to obtain accurate measurements at low pressures ($P'<0.1$ Torr) and at high pressures ($P'>3$ Torr). At low pressures, a negligibly quenching buffer gas ($\sim$0.5 Torr of He) was added to CO in order to limit the diffusion of the fluorescing molecules out of the detection solid angle, thereby avoiding the artifact of a subnatural lifetime. At high pressures, the laser excitation energy was reduced by means of neutral density filters because the fluorescence signal departed significantly from a single-exponential decay when using full laser energy. This effect is illustrated in Fig. 6 showing the initial decay of the fluorescence induced in $\sim$4 Torr of CO by a 3.6, 18, and 36 μJ energy laser pulse (for a better comparison, the recorded traces are suitably rescaled). While for 3.6 μJ excitation the signal is well described by a single exponential, at higher pulse energies an initial, rapidly falling component appears. The nonexponential decay was more evident at higher CO pressures, while it was undetectable for $P'<0.1$ Torr. A similar behavior as a function of the laser excitation energy was observed by Stacewicz *et al.* in fluorescence from sodium vapor[35] and explained as resulting from a temporary reduction of the radiation-trapping efficiency due to optical pumping of the ground-state population in the absorbing atoms.[36] This picture, however, does not apply in our case since the laser beam excites only a very small fractional volume of the CO molecules present in the cell. Also, Swan-band emission from photoproduced C_2 is ruled out as a possible explanation since it was only observed at CO pressures above $\sim$25 Torr,[7,8] and it is known to have a longer lifetime than CO $B\,^1\Sigma^+$ ($v'=0$).[7] Instead, we attributed the effect to the action of $B\rightarrow A$ SE. To corroborate this interpretation, we detected the SE emerging collinearly with the laser beam

TABLE I. Quenching rate coefficients, q, and corresponding quenching cross sections, σ, of CO $B\,^1\Sigma^+$ ($v'=0$) in collisions with the investigated quenching species.

		σ (Å^2)	
Quencher	q (MHz Torr^{-1})	This work	Previous studies
H_2O	42±2	170±8	
C_3H_8	29.1±1.5	144±7	
CO_2	26±1	133±5	
CH_4	21±1	81±4	
O_2	18±1	85±5	
Xe	17±1	99±6	
Kr	7.6±0.2	42±2	
H_2	6.6±0.2	11.0±0.4	10.7±0.7[b] 20.8±1[c]
Ar	5.6±0.1	27.7±0.5	22.4±2[b]
N_2	5.4±0.1	24.6±0.5	20.5[a]
Ne	0.13±0.01	0.54±0.04	0.48±0.2[b]
He	0.11±0.01	0.25±0.02	0.23±0.8[b] <0.5[c]

[a]Reference 1.
[b]Reference 17.
[c]Reference 18.

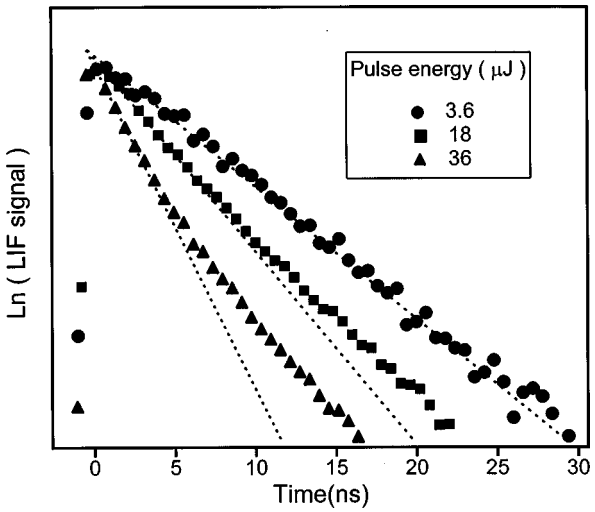

FIG. 6. Two-photon LIF signals from $\sim$4 Torr of pure CO obtained with different laser-pulse energies (see the text).

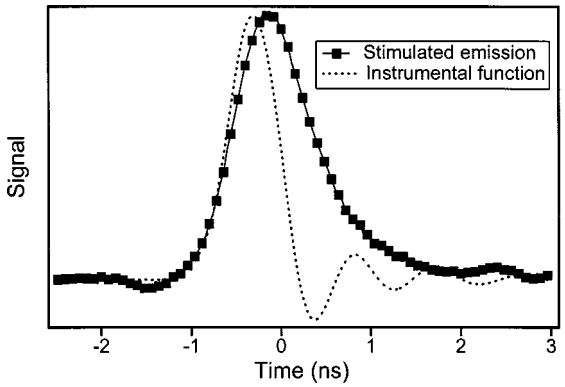

FIG. 7. Stimulated emission from ~4 Torr of pure CO. The laser-pulse energy was ~36 μJ.

simultaneously with the fluorescence emitted at 90° from ~4 Torr of CO. The time-resolved SE signal, shown in Fig. 7, is characterized by a temporal width $\gtrsim$1 ns (FWHM), which demonstrates that significant SE occurs during the initial part of the fluorescence decay. SE can provide an important depopulation channel for the B state, thereby affecting the dynamics of the fluorescence from B. In addition, the SE cross section is proportional to the B-A population inversion, which, in turn, increases with optical population of the $X \rightarrow \rightarrow B$ transition, consistent with the observed pulse-energy dependence of the effect.

To use the model developed in Sec. III for analyzing the lifetime measurements of Fig. 5, the pressure dependence of K must be assessed. To this end, we note that, while the room-temperature Doppler width of $B \leftrightarrow X$ transitions is about 0.2 cm^{-1}, the collisional width increases from $\sim 10^{-6}$ to $\sim 10^{-2}$ cm^{-1} as P' increases from ~0.001 to ~8 Torr, as calculated from the pressure-broadening coefficients of Di Rosa and Farrow.[37] At $P' = P'_{max}$, however, the collisional width is still about three orders of magnitude less than the Doppler width. Hence, in the entire trapping-dominated regime, namely $0 < P' \lesssim P'_{max}$, the broadening mechanism is predominantly inhomogeneous. On the other hand, at pressures where the collisional width becomes comparable to the Doppler width ($P' > 10$ Torr), the dynamics of the excited-state population is driven mainly by quenching such that errors in modeling the radiation trapping become less critical. In light of these considerations, we assume that the lineshape is Doppler broadened over the pressure range of Fig. 5 and take K as proportional to the number density of the ground-state CO molecules. Thus, in ideal gas conditions, $K = \alpha P'$.[38] Based on this assumption, we have fitted the expression for the effective lifetime given in Eq. (6) (with $m = 0$) to the observations, using a Levenberg–Marquardt fitting routine and treating τ_{rad}, Q, β, and α as fitting parameters. As seen in Fig. 5, the model faithfully reproduces the observed variation of fluorescence lifetime as a function of the CO pressure. The fit results are summarized in Table II and the uncertainties are estimated based on standard deviations from multiple measurements, statistical fitting errors, and nominal accuracy of the model for $\tilde{g}_0$ as provided by Ref. 32.

TABLE II. Radiative lifetime of a CO $B\,^1\Sigma^+$ ($v' = 0$), self-quenching rate coefficient and cross section, and the branching ratio for the $B\,^1\Sigma^+ \rightarrow X\,^1\Sigma^+$ fluorescence channel obtained from the fit shown in Fig. 5. The Einstein coefficients for the $B\,^1\Sigma^+ \rightarrow A\,^1\Pi$ and $B\,^1\Sigma^+ \rightarrow X\,^1\Sigma^+$ fluorescence channels are given by $A_{B\rightarrow X} = \beta/\tau_{rad}$, and $A_{B\rightarrow A} = (1-\beta)/\tau_{rad}$, respectively.

	This work	Previous studies
τ_{rad} (ns)	22.3±0.5	29.8±1.2[d]
		20.8±1.0[e]
		23±3[g]
		22.2[h]
q (MHz Torr^{-1})	8.1±0.4	5.9[a]
		7.8[b]
		7.9[c]
		7.9[h]
σ (Å^2)	37±2	
β	0.7±0.1	0.68±0.5[g]
		0.7[h]
$A_{B\rightarrow X}$ (MHz)	31±5	19±1[d]
		30±6[g]
$A_{B\rightarrow A}$ (MHz)	13±2	14.5±0.6[d]
		13.9±0.6[g]
		13.4[h]

[a]Reference 1.
[b]Reference 7.
[c]Reference 9.
[d]Reference 24.
[e]Reference 25.
[f]Reference 35.
[g]Reference 45.
[h]Reference 46.

V. DISCUSSION

A full theoretical understanding of quenching rates relies on the knowledge of the potential energy surfaces for the colliding molecules and may require considerable computational efforts. However, useful analyses of excited-state quenching have been performed using models based on a less detailed quantum-mechanical approach.[39,40] A starting point for the analysis of $B\,^1\Sigma^+$ quenching can be drawn, for example, from results concerning the well-characterized NO $A\,^2\Sigma^+$ state, which is also a $3s\sigma$ Rydberg state and possesses a relatively similar dipole moment[24,41] and polarizability.[42] Haas *et al.*[40] and, later, Paul *et al.*,[41] showed that quenching of NO $A\,^2\Sigma^+$ by a variety of collision partners (M) can be understood in terms of a ''harpoon'' mechanism. According to this description, the covalent, NO (A)–M, and ionic, NO^+-M^-, potential energy surfaces cross at a certain intermolecular distance and the Rydberg electron is transferred to the colliding species. This process constitutes the entrance channel for quenching. The exit channel occurs when the electron returns to NO at the crossing between the ionic surface and the covalent NO(X)–M surface.

A major difficulty is immediately found in adapting this picture to CO $B\,^1\Sigma^+$. According to the harpoon model, the cross sections for quenching by species with unstable negative ions, i.e., ions subject to rapid autodetachment on the collisional time scale, is expected to be near zero. Among these species are noble gases, H_2, and saturated hydrocarbons such as CH_4 and C_3H_8,[41] which, in contradiction with the harpoon-model predictions, are very efficient quenchers

of CO $B\,^1\Sigma^+$ (with the exception of Ne and He). Thus, the harpoon process cannot be invoked as the (only) quenching mechanism for CO $B\,^1\Sigma^+$. Other processes are known to result in collisional removal from CO $B\,^1\Sigma^+$ $(v'=0)$, such as its propensity for collision-induced intersystem crossing (CIISC)[43] to nearly isoenergetic $b\,^3\Sigma^+$ $(v=0,1)$ triplet states. The presence of CIISC is inferred from the observation of collision-induced $b\,^3\Sigma^+ \rightarrow a\,^3\Pi$ fluorescence in the third positive system (260–360 nm) following two-photon excitation of the $B\,^1\Sigma^+$ $(v'=0)$ state.[1,7,8,44] We have also monitored the pressure dependence of buildup and decay times of the $b\,^3\Sigma^+ \rightarrow a\,^3\Pi$ triplet fluorescence induced by collisions with each quenching species under investigation. While these measurements and their analysis will be the subject of a future publication, immediate results relevant to the present study are that triplet fluorescence was observed for every quencher gas and that the buildup time was comparable in each case to the decay time of the $B\,^1\Sigma^+ \rightarrow A\,^1\Pi$ fluorescence. This result suggests that CIISC is, indeed, an active quenching channel for CO $B\,^1\Sigma^+$ $(v'=0)$. In addition, some of the large quenching cross sections measured in our experiment (in particular, those for H_2O, C_3H_8, CO_2, CH_4, O_2, and CO) can reflect additional contributions from resonance energy transfer,[19] i.e., the transfer of energy mediated by the exchange of a virtual photon between the electronically excited CO and collision partners featuring significant absorption at 115 nm.[45]

A further discussion of specific cases is given in the following, along with comparisons to CO quenching measurements appearing in the literature.

A. Quenching by noble gases

Given the discussed inefficiency of the harpoon mechanism and the absence of resonant transitions at 115 nm for noble gases, the significant CO $B\,^1\Sigma^+$ quenching cross sections for collisions with Ar, Kr, and Xe should be entirely due to CIISC, in agreement with the conclusions of Comes and Fink.[17] These authors published results for Ne and He in excellent quantitative agreement with ours, while their cross section for quenching by Ar is slightly smaller. Note, however, that their use of Stern–Volmer techniques may introduce systematic errors, as discussed in Sec. I, resulting in larger uncertainties than ours. In a later study, Dimov and Vidal[18] reported an upper limit of 0.5 Å^2 for the cross section of quenching by He, which is also consistent with our measured value. In Ref. 46, Kleiman *et al.* quoted an unpublished study according to which the cross sections for quenching by Kr and Xe were measured to be gas kinetic, while those of He, Ne, and Ar were too small to be detected. These findings agree well with ours based on comparisons to cross sections for quenching by Kr, He, and Ne. Discrepancies appear, instead, for Xe (our measured cross section is larger than the gas-kinetic value[47]) and Ar (our measured cross section exceeds those of He and Ne by about two orders of magnitude). The authors do not specify, however, the relative uncertainty of the quoted measurements, which was probably rather large since the result for Ar is described as in qualitative agreement with that of Comes and Fink.[17] Finally, quenching by Ne is qualitatively discussed in Ref. 8, where Westblom *et al.* argue that the corresponding cross section may be smaller than that for N_2, which is confirmed by our measurements.

B. Quenching by molecular species

As mentioned above, resonance energy transfer is likely to play an important role for several molecular quenchers. Moreover, H_2O, CO_2, O_2, and CO are known to have relatively stable negative ions[41] and, therefore, could potentially quench CO $B\,^1\Sigma^+$ through all available mechanisms, making a theoretical prediction of quenching cross sections for such species particularly difficult.

To our knowledge, no experimental result nor prediction has been reported for quenching of CO $B\,^1\Sigma^+$ by H_2O, CO_2, O_2, and hydrocarbons. In Ref. 9, Agrup and Aldén briefly discuss the quenching by CO_2 in a room-temperature flow and conclude that the quenching rate coefficient for CO_2 is slightly larger than that for CO self-quenching, consistent with our results. Quenching by N_2 has been studied by Loge *et al.*,[1] who obtained a quenching cross section of 20.5 Å^2, in reasonable agreement with our result (no uncertainty is provided for their measurement). Finally, Comes and Fink[17] investigated the quenching by H_2 and obtained a cross section in excellent agreement with ours, but in substantial disagreement with later results of Dimov and Vidal.[18] The latter authors, however, adopted a doubly resonant scheme to reach CO $B\,^1\Sigma^+$ through an intermediate transition to the $A\,^1\Pi$ state and then analyzed their data using Stern–Volmer plots. Population losses at the intermediate stage of the excitation were accounted for, but undoubtedly introduced additional uncertainty.

C. Self-quenching, radiative lifetime, and SE

Although the radiation trapping of the $B \rightarrow X$ fluorescence in CO is a well-known phenomenon, no quantitative modeling of its effects on the dynamics of the $B \rightarrow A$ fluorescence emission has been reported. To our knowledge, only Carlson and co-workers[29] published a semiempirical analysis of the trapping effect, using the theoretical treatment of Holt[38] to describe the pressure dependence of the CO $B\,^1\Sigma^+$ $(v'=0)$ lifetime measured with a time-resolved electron-beam technique. The approximations in their model were, however, significant and, in fact, a substantial disagreement with the observed lifetimes for CO pressures above ~6 mTorr was apparent. Typically, the radiative trapping in CO is modeled by extrapolation to zero pressure. Experimental findings similar to ours were published by Dotchin *et al.*,[48] who time resolved the CO $B\,^1\Sigma^+$ $(v'=0)$ emission with a photon-coincidence technique following excitation by a pulsed proton beam, and, more recently, by Bergström *et al.*,[49] who used two-photon LIF with a nanosecond dye laser. In both works, τ_{rad} was estimated by extrapolating the lifetime measurements to zero pressure. The Einstein coefficient for the $B \rightarrow A$ spontaneous emission (hence, β) was obtained from the zero-pressure intercept of a straight line fitting the γ vs P' curve, assumed to be fully trapped. From the slope of this straight line, Bergström *et al.* determined also the self-quenching rate coefficient. As

shown in Table II, those results are in excellent agreement with ours. Other estimates of self-quenching rate coefficient are reported by Agrup and Aldén,[9,10] who used time-resolved LIF, and Loge *et al.*,[1] who used nanosecond laser excitation and Stern–Volmer plots for an analysis. As can be seen from Table II, the Agrup's result is in excellent agreement with ours, while the Loge's value is slightly lower (although the uncertainty is not given) probably because of the difficulty in assessing the extent of radiative trapping. A similar difficulty appears occasionally even in more recent reports. In Ref. 18, Dimov and Vidal describe experiments in a cell by which they detect VUV $B \rightarrow X$ fluorescence and, without specifying the CO partial pressure, state that the fluorescence was not affected by radiation trapping. This is possible only if trace-level (<1 mTorr) amounts of CO were used, which is inconsistent with the description of their experiment. Neglecting radiative trapping results in an overestimation of the lifetime. This could partly explain the substantial disagreement between their estimate of the quenching cross section by H_2 and that reported by Comes and Fink,[17] as well as with our result. In Ref. 24, Drabbels and co-workers reported a value for the $B\,^1\Sigma^+$-state radiative lifetime (29.8 ± 1.2 ns), which appears to be inflated by residual trapping. They assume that trapping was avoided by using a mixture of 2% CO in argon, implying that the dilution of CO in a buffer gas reduces trapping. In the Doppler limit, however, the trapping effect depends only on the number density of ground-state CO molecules along the emitted photon path and, therefore, only on the CO partial pressure. If collisional broadening by argon was significant, the radiation trapping would have been reduced.[17] According to our measured quenching cross sections and results in Ref. 37 though, quenching by argon would have dominated the dynamics of the *B*-state population.

Our estimate of τ_{rad} agrees with the results of previous measurements, which, in our judgment, properly accounted for trapping effects. These are compiled in Table II for a comparison (for a more extensive account of earlier results, see, for example, Ref. 50).

The $B \rightarrow A$ SE has been extensively studied.[8,49,51] In our experiment, SE was visible to the eye for CO pressures above 3 Torr and pulse energies >10 μJ. It was detectable using the PIN photodiode down to ~1 Torr with pulse energies ~100 μJ. The interplay between SE and the detected fluorescence was, also, explicitly addressed by Westblom *et al.*,[8] and Bergström *et al.*,[49] who investigated the effect of SE on the temporal decay of the fluorescence emission in the case of nanosecond-pulse excitation.

VI. CONCLUSIONS

We performed direct measurements of room-temperature quenching cross sections of CO $B\,^1\Sigma^+$ ($v'=0$) in collisions with H_2O, C_3H_8, CO_2, CH_4, O_2, Xe, CO, Kr, H_2, Ar, N_2, Ne, and He by using time-resolved, two-photon LIF with a picosecond laser. Quantitative results for H_2O, C_3H_8, CO_2, CH_4, O_2, Xe, and Kr are reported for the first time, to our knowledge. A theoretical treatment for the radiative trapping of the $B \rightarrow X$ fluorescence is presented and is used to develop a quantitative model for the pressure dependence of the *B*-state decay rate. The model accurately reproduces the observed fluorescence lifetimes of neat CO and was used, in particular, to determine the CO self-quenching. A consideration of mechanisms consistent with our results suggests that quenching of CO $B\,^1\Sigma^+$ ($v'=0$) is more complex than the previously characterized quenching of OH $A\,^2\Sigma^+$ ($v=0$)[52] and NO $A\,^2\Sigma^+$ ($v=0$)[41] and can proceed through several deactivation channels, including collision-induced intersystem crossing, intermolecular resonance energy transfer, and harpooning.

The measurement of collider-specific quenching cross sections can provide further insight into the nature of the intermolecular interactions involving CO and can aid in the development of a reliable and complete quenching model for an analysis of LIF measurements of CO. To this end, an extension of the present work will be the study of the temperature dependence of the species-specific quenching cross sections, which is currently underway in our laboratory.

ACKNOWLEDGMENTS

This work was supported by the U.S. Department of Energy, Office of Basic Energy Sciences, Chemical Sciences Division. The authors acknowledge the expert technical assistance of Paul E. Schrader, Sandia National Laboratories. F. Di Teodoro thanks Professor Andreas Mölisch, Vienna University of Technology, and Dr. Francesco Fuso, University of Pisa, for helpful discussions of radiation trapping.

[1] G. W. Loge, J. J. Tiee, and F. B. Wampler, J. Chem. Phys. **79**, 196 (1983); see also J. J. Tiee, M. J. Ferris, G. W. Loge, F. B. Wampler, and A. Hartford, Laser Insti. Am. **34**, 53 (1982).
[2] J. Haumann, J. M. Seitzman, and R. K. Hanson, Opt. Lett. **11**, 776 (1986).
[3] J. M. Seitzman, J. Haumann, and R. K. Hanson, Appl. Opt. **26**, 2892 (1987).
[4] D. L. Van Oostendorp, W. T. Borghols, and H. B. Levinsky, Combust. Sci. Technol. **79**, 195 (1991).
[5] D. A. Everest, C. R. Shaddix, and K. C. Smyth, *26th Symposium (International) on Combustion* (The Combustion Institute, Pittsburgh, PA, 1996), p. 1161.
[6] N. Georgiev and M. Aldén, Appl. Spectrosc. **51**, 1229 (1997).
[7] M. Aldén, S. Wallin, and W. Wendt, Appl. Phys. B: Photophys. Laser Chem. **33**, 205 (1984).
[8] U. Westblom, S. Agrup, M. Aldén, H. M. Hertz, and J. E. M. Goldsmith, Appl. Phys. B: Photophys. Laser Chem. **50**, 487 (1990).
[9] S. Agrup and M. Aldén, Chem. Phys. Lett. **189**, 211 (1992).
[10] S. Agrup and M. Aldén, Appl. Spectrosc. **48**, 1118 (1994).
[11] A. V. Mokhov, H. B. Levinsky, C. E. van der Meij, and R. A. A. M. Jacobs, Appl. Opt. **34**, 7074 (1995).
[12] A. P. Nefedov, V. A. Sinel'shchikov, A. D. Usachev, and A. V. Zobnin, Appl. Opt. **37**, 7729 (1998).
[13] A. V. Zobnin, A. P. Nefedov, V. A. Sinel'shchikov, and A. D. Usachev, Opt. Spectrosc. **87**, 23 (1999).
[14] G. J. Fiechtner, C. D. Carter, and R. S. Barlow, *Proceedings of the 33rd National Heat Transfer Conference*, 15–17 August, 1999, Albuquerque, New Mexico, p. 1.
[15] L. Gasnot, P. Desgroux, J. F. Pauwels, and L. R. Sochet, Combust. Flame **117**, 291 (1999).
[16] A. V. Mokhov, A. P. Nefedov, B. V. Rogov, V. A. Sinel'shchikov, A. D. Usachev, A. V. Zobnin, and H. B. Levinsky, Combust. Flame **119**, 161 (1999).
[17] F. J. Comes and E. H. Fink, Z. Naturforsch. **28a**, 717 (1973).
[18] S. S. Dimov and C. R. Vidal, Chem. Phys. Lett. **221**, 307 (1994).
[19] J. T. Yardley, *Introduction to Molecular Energy Transfer* (Academic, New York, 1980).
[20] X. Ma and R. Lai, Phys. Rev. A **49**, 787 (1993).

[21] N. D. Hung, Y. Segawa, Y. H. Meyer, P. Long, and L. H. Hai, Appl. Phys. B: Photophys. Laser Chem. **62**, 449 (1996).
[22] H. Rottke and H. Zacharias, Opt. Commun. **55**, 87 (1985).
[23] P. J. H. Tjossem and K. C. Smyth, J. Chem. Phys. **91**, 2041 (1989).
[24] M. Drabbels, W. L. Meerts, and J. J. ter Meulen, J. Chem. Phys. **99**, 2352 (1993).
[25] The parameters for calculating the spectrum of the two-photon absorption cross section were taken from M. D. Di Rosa and R. L. Farrow, J. Opt. Soc. Am. B **16**, 1988 (1999).
[26] The laser frequency was tuned to maximize the fluorescence signal prior to the measurements. This procedure brings the center of the laser lineshape to roughly coincide with the $Q(5)$ two-photon transition, as calculated convolving the laser lineshape with the two-photon absorption cross section.
[27] D. J. Hart and O. L. Bourne, Chem. Phys. **133**, 103 (1989).
[28] Rotational-level-dependent quenching has been observed in some molecules, e.g., OH $A\,^2\Sigma^+$ [see R. A. Copeland, M. J. Dyer, and R. Crosley, J. Chem. Phys. **82**, 4022 (1985)]. In other molecules, e.g., NO $A\,^2\Sigma^+$, such an effect has not been detected, as discussed in J. A. Gray, P. H. Paul, and J. L. Durant, Chem. Phys. Lett. **190**, 266 (1992). A further study of rotational dependence in the quenching of CO $B\,^1\Sigma^+$ is underway in our laboratory.
[29] T. A. Carlson, N. Duric, P. Erman, and M. Larsson, Z. Phys. A **287**, 123 (1978).
[30] J. H. Moore and D. W. Robinson, J. Chem. Phys. **48**, 4870 (1968).
[31] T. Holstein, Phys. Rev. **72**, 1212 (1947); **83**, 1159 (1951).
[32] A. F. Mölisch and B. P. Ohery, *Radiation Trapping in Atomic Vapors* (Clarendon, Oxford, 1999).
[33] A. F. Mölisch, B. P. Ohery, and G. Magerl, J. Quantum Spectrosc. Radiat. Transf. **48**, 377 (1992); A. F. Mölisch, B. P. Ohery, W. Schupita, and G. Magerl, *ibid.* **49**, 361 (1993).
[34] A. F. Mölisch, B. P. Ohery, W. Schupita, and G. Magerl, J. Phys. B **30**, 1879 (1997).
[35] J. Chorąży, T. Kotowski, and T. Stacewicz, Opt. Commun. **125**, 65 (1996).
[36] N. N. Bezuglov, A. N. Klucharev, A. F. Mölisch, M. Allegrini, F. Fuso, and T. Stacewicz, Phys. Rev. A **55**, 3333 (1997).
[37] M. D. Di Rosa and R. L. Farrow, J. Quantum Spectrosc. Radiat. Transfer (in press).
[38] H. K. Holt, Phys. Rev. A **13**, 1442 (1976).
[39] See, for example, C. A. Thayer, and J. T. Yardley, J. Chem. Phys. **57**, 3992 (1972); H.-M. Lin, M. Seaver, K. Y. Tang, A. E. W. Knight, and C. S. Parmenter, *ibid.* **70**, 5442 (1979).
[40] M. Asscher and Y. Haas, J. Chem. Phys. **76**, 2115 (1982); Y. Haas and G. D. Greenblatt, J. Phys. Chem. **90**, 513 (1986).
[41] P. H. Paul, J. A. Gray, J. L. Durant, and J. W. Thoman, Appl. Phys. B: Photophys. Laser Chem. **57**, 249 (1993).
[42] See discussions in M. D. Di Rosa and R. K. Hanson, J. Mol. Spectrosc. **164**, 97 (1994) and in Ref. 37.
[43] K. F. Freed, Adv. Chem. Phys. **47**, 291 (1981).
[44] L. F. DiMauro and T. A. Miller, Chem. Phys. Lett. **138**, 175 (1987).
[45] H. Okabe, *Photochemistry of Small Molecules* (Wiley, New York, 1978).
[46] V. Kleiman, K. Trentelman, Y. Huang, and R. J. Gordon, Chem. Phys. Lett. **222**, 161 (1994).
[47] The gas-kinetic cross section for quenching by Xe was estimated by assuming the rigid-sphere approximation. The Lennard-Jones radius of Xe (4.3 Å) was taken from the appendix of J. O. Hirschfelder, C. F. Curtiss, and R. B. Bird, *Molecular Theory of Gases and Liquids* (Wiley, New York, 1954). The Lennard-Jones radius of CO $B\,^1\Sigma^+$ was assumed to be 20% larger than the ground-state value (3.9 Å) obtained from the same reference.
[48] L. W. Dotchin, E. L. Chupp, and D. J. Pegg, J. Chem. Phys. **59**, 3960 (1973).
[49] H. Bergström, H. Lundberg, and A. Persson, Z. Phys. D: At., Mol. Clusters **21**, 323 (1991).
[50] E. Krishnakumar and S. K. Srivastava, Astrophys. J. **307**, 795 (1986).
[51] J. J. Tiee, C. R. Quick, G. W. Loge, and F. B. Wampler, J. Appl. Phys. **63**, 288 (1988).
[52] See P. H. Paul, J. Quant. Spectrosc. Radiat. Transf. **51**, 511 (1994), and references therein.